First-Generation Chiral Metallodendrimers: Stereoselective Synthesis of Rigid *D*₃-Symmetric Tetranuclear Ruthenium Complexes

Swamy Bodige, Andrew S. Torres, David J. Maloney, David Tate, Gary R. Kinsel, Angela K. Walker, and Frederick M. MacDonnell*

Contribution from the Department of Chemistry and Biochemistry, The University of Texas at Arlington, Arlington, Texas 76019

Abstract: Condensation reactions between the enantiopure, substitutionally inert building blocks Δ-[Ru(1,10-phenanthroline-5,6-dione)₃][PF₆]₂ (**2**) and Δ-[Ru(phen)₂(1,10-phenanthroline-5,6-diamine)][PF₆]₂ (**3**) gave the *D*₃-symmetric tetramer [(Δ-(phen)₂Ru(tpphz))₃-Δ-Ru]⁸⁺ (ΔΔ₃-**1**) in 68% isolated yield as the PF₆⁻ salt (where tpphz is tetrapyrido[3,2-*a*:2′,3′-*c*:3″,2″-*h*:2″,3″-*j*]phenazine). Reactions between appropriate enantiomers of **2** and **3** also yielded the remaining *D*₃ isomers ΛΔ₃-**1**, ΔΛ₃-**1**, and ΛΛ₃-**1** which collectively represent the highest nuclearity Ru oligomers based on bidentate type ligands prepared in a stereospecific fashion to give diasteromerically and enantiomerically pure products. The complexes were purified via cation-exchange HPLC. ¹H and ¹³C NMR, COSY and HMQC NMR, and UV−visible spectroscopy were employed to characterize these supramolecular assemblies. MALDI-TOF mass spectrometry gave parent molecular ion peaks corresponding to the species *m/z* 2638 [**1** − 8PF₆]⁺, 2783 [**1** − 7PF₆]⁺, 2928 [**1** − 6PF₆]⁺, 3073 [**1** − 5PF₆]⁺, 3218 [**1** − 4PF₆]⁺, and 3363 [M − 3PF₆]⁺, proving the macromolecular structure. Circular dichroism spectroscopy was used to determine the absolute stereochemistry and optical purity of each of these stereoisomers.

Dendrimers, a class of hyperbranched nanosized molecules,[1−3] offer unique architectures in which to organize multiple chromophores or redox centers into precisely defined and highly symmetric structures. Recently, much attention has been focused on the incorporation of luminescent, redox-active, transition-metal complexes, such as ruthenium polypyridine species, into the dendrimer structure as the potential of such systems for applications in light harvesting and energy storage devices was quickly realized.[4−6] The antenna-like structure of the dendrimer provides an ideal organization for these chromophores and redox centers to work in synergistic ways.[7−9] For example, redox-active dendritic structures containing from 4 to 22 tris-diimine metal complexes have been isolated, many of which exhibit luminescence with appreciable room temperature lifetimes in solution and light-induced antenna-effect energy transfer.[10−25]

A less-explored but equally exciting aspect of these metallodendrimers concerns the stereochemistry of these supramolecules. Metallodendrimers constructed of *D*₃-symmetric [M(diimine)₃]²⁺ units[10−25] exhibit tremendous stereochemical complexity arising from the local chirality (Δ or Λ) of each metal center. While problematic in that stereospecific syntheses have been lacking until recently,[26−31] the controlled incorporation of these chiral structural elements into the dendritic structure

* Author to whom correspondence should be addressed.
⊗ Abstract published in *Advance ACS Abstracts,* October 15, 1997.
(1) Tomalia, D. A.; Naylor, A. M.; Goddard, W. A. *Angew. Chem., Int. Ed. Engl.* **1990,** *29,* 138.
(2) Newkome, G. R.; Moorefield, C. N. In *Advances in Dendridic Macromolecules*; Newkome, G. R., Ed.; JAI Press: Greenwich, CT, 1994; Vol. 1, p 1.
(3) Frechét, J. M. *Science* **1994,** *263,* 1710.
(4) Balzani, V.; Scandola, F. *Supramolecular Photochemistry*; Horwood: Chichester, U.K., 1991.
(5) Balzani, V.; Juris, A.; Venturi, M.; Campagna, S.; Serroni, S. *Chem. Rev.* **1996,** *96,* 759.
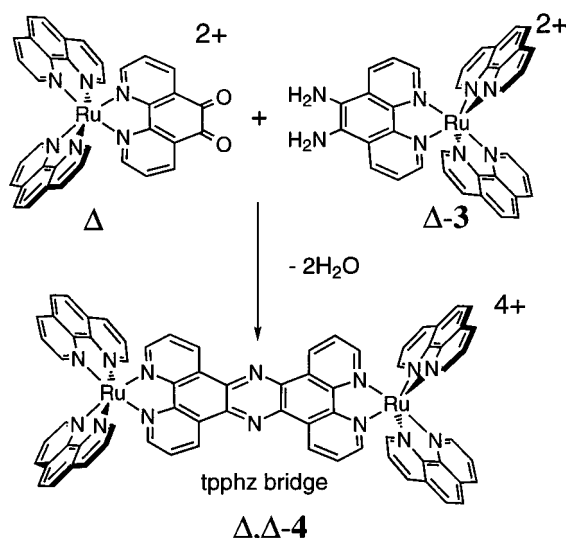(6) Lehn, J.-M. *Supramolecular Chemistry, Concepts and Perspectives*; VCH: New York, 1995.
(7) Denti, G.; Campagna, S.; Serroni, S.; Juris, A.; Ciano, M.; Balzani, V. In *Perspectives in Coordination Chemistry*; Williams, A. F., Floriani, C., Merbach, A. E., Eds.; VCH: Basel, Switzerland, 1992; p 153.
(8) Denti, G.; Campagna, S.; Balzani, V. In *Mesomolecules: From Molecules to Materials*; Mendenhall, D., Greensburg, A., Liebman, J., Eds.; Chapman and Hall: New York, 1995; p 69.
(9) Scandola, F.; Argazzi, R.; Bignozzi, C. A.; Chiorboli, C.; Indelli, M. T.; Rampi, M. A. In *Supramolecular Chemistry*; Balzani, V., De Cola, L., Eds.; Kluwer Academic Publishers: The Netherlands, 1992; p 235.

(10) Campagna, S.; Denti, G.; Serroni, S.; Juris, A.; Venturi, M.; Ricevuto, V.; Balzani, V. *Chem. Eur. J.* **1995,** *1,* 211.
(11) Serroni, S.; Juris, A.; Campagna, S.; Venturi, M.; Denti, G.; Balzani, V. *J. Am. Chem. Soc.* **1994,** *116,* 9086.
(12) Juris, A.; Balzani, V.; Campagna, S.; Denti, G.; Serroni, S.; Frei, G.; Güdel, H. U. *Inorg. Chem.* **1994,** *33,* 1491.
(13) Serroni, S.; Denti, G.; Campagna, S.; Juris, A.; Ciano, M.; Balzani, V. *Angew. Chem., Int. Ed. Engl.* **1992,** *31,* 1493.
(14) Serroni, S.; Denti, G. *Inorg. Chem.* **1992,** *31,* 4251.
(15) Denti, G.; Campagna, S.; Serroni, S.; Ciano, M.; Balzani, V. *J. Am. Chem. Soc.* **1992,** *114,* 2944.
(16) Campagna, S.; Denti, G.; Serroni, S.; Ciano, M.; Balzani, V. *Inorg. Chem.* **1991,** *30,* 3728.
(17) Denti, G.; Campagna, S.; Sabatino, L.; Serroni, S.; Ciano, M.; Balzani, V. *Inorg. Chem.* **1990,** *29,* 4750.
(18) Schemehl, R. H.; Auerbach, R. A.; Wacholtz, W. F.; Elliott, C. M.; Freitag, R. A.; Merket, J. W. *Inorg. Chem.* **1986,** *25,* 2440.
(19) Murphy, J. W. R.; Brewer, K. J.; Gettliffe, G.; Petersen, J. D. *Inorg. Chem.* **1989,** *28,* 81.
(20) Hunziker, M.; Lüdi, A. *J. Am. Chem. Soc.* **1977,** *99,* 7370−7371.
(21) Moucheron, C.; Kirsch-DeMesmaeker, A.; Dupont-Gervais, A.; Leize, E.; Van Dorsselaer, A. *J. Am. Chem. Soc* **1996,** *118,* 12834.
(22) Haga, M.; Ali, M. M.; Arakawa, R. *Angew. Chem., Int. Ed. Engl.* **1996,** *35,* 76.
(23) Arakawa, R.; Matsuo, T.; Nozaki, K.; Ohno, T.; Haga, M. *Inorg. Chem.* **1995,** *34,* 2464.
(24) Marvard, V.; Astrue, D. *Chem. Commun.* **1997,** 773.
(25) Cleary, R. L.; Byrom, K. J.; Bardwell, D. A.; Jeffery, J. C.; Ward, M. D.; Calogero, G.; Armaroli, N.; Flamigni, L.; Barigelletti, F. *Inorg. Chem.* **1997,** *36,* 2601.
(26) MacDonnell, F. M.; Bodige, S. *Inorg. Chem.* **1996,** *35,* 5758.
(27) Hua, X.; von Zelewsky, A. *Inorg. Chem.* **1991,** *30,* 3796.
(28) Hua, X.; von Zelewsky, A. *Inorg. Chem.* **1995,** *34,* 5791.
(29) Wärnmark, K.; Heyke, O.; Thomas, J. A.; Lehn, J.-M. *Chem. Commun.* **1996,** 2603.
(30) Wärnmark, K.; Thomas, J. A.; Heyke, O.; Lehn, J.-M. *Chem. Commun.* **1996,** 701.
(31) Tzalis, D.; Tor, Y. *J. Am. Chem. Soc.* **1997,** *119,* 852.

First-Generation Chiral Metallodendrimers

J. Am. Chem. Soc., Vol. 119, No. 43, 1997 10365

Scheme 1

presents an opportunity to fine tune the stereochemistry of these supramolecules and possibly expand their utility to include roles as host complexes for chiral molecular recognition. Furthermore, it would considerably simplify the characterization of these multinuclear complexes as the diastereomeric mixtures generated (when stereochemical control is lacking) often preclude NMR and crystallographic characterization and complicate interpretation of the photophysical and electrochemical data. Metallodendrimers constructed from tridentate polypyridine ligands,[24,32−36] such as terpy derivatives, avoid these problems owing to the basic stereochemistry of the building blocks (D_2-symmetric [M(terpy)$_2$]$^{2+}$ units);[37] however, interest in terpy-based oligomers is restricted by the absence of room temperature luminescence of [Ru(terpy)$_2$]$^{2+}$, their basic chromophoric component,[5,38,39] which makes them less suitable for many practical applications involving light-induced processes. The achiral geometry similarly limits their potential to act as host complexes for chiral molecular recognition. Clearly, efficient methods for the stereospecific syntheses of multinuclear complexes containing chiral [M(diimine)$_3$]$^{2+}$ units are desirable for further progress in this field.

Recently, we reported a new approach toward the stereospecific syntheses of multinuclear complexes which utilizes enantiopure, substitutionally inert ruthenium tris-diimine complexes as molecular building blocks.[26] Linking functions at the periphery of the coordinated ligands are used to join inert complexes. As shown in Scheme 1, this method of oligomer construction does not involve making or breaking bonds at the metal stereocenter. This approach fundamentally differs from stereospecific syntheses that rely on ligand displacement reactions at the chiral center, such as reactions of enantiopure *cis*-[Ru(phen)$_2$(py)$_2$]$^{2+}$, *cis*-[Ru(bpy)$_2$(py)$_2$]$^{2+}$,[27,29] and *cis*-[Ru-

(phen)$_2$(CO)$_2$]$^{2+}$.[40] Oligonuclear assemblies based on these complexes must rely on multitopic ligands, such as HAT and PHAT,[29,41,42] to serve as the branching site because only one bidentate site (two *cis* coordination sites) is available for bridging. In our system, the central pyrazine ring forms in high yield to give a rigid, aromatic, and irreversible tpphz bridge (tpphz is tetrapyrido[3,2-*a*:2′,3′-*c*:3″,2″-*h*:2‴,3‴-*j*]phenazine) between stereocenters. Acetylenic bridges[31,43] and square-planar metal complex bridges[30] have also been used to join chiral, inert ruthenium tris-diimine complexes. Similarly, ether functions have been used to join properly derivatized [Ru(terpy)$_2$]$^{2+}$ complexes.[34−36] The various bridging functions provide different degrees of conformational flexibility, chemical stability, and electronic communication between the metal centers. For electronic communication (energy-transfer applications) and conformational stability (molecular recognition applications), the phenazine bridge has distinct advantages. In this report, we extend this bridging reaction along each 2-fold axis of the D_3-symmetric building block, [Ru(phendione)$_3$]$^{2+}$, to build rigid, enantiopure, "metal-centered" first-generation metallodendrimers of unusually high symmetry and nanoscopic chirality. The synthesis and characterization of four nanoscopic D_3-symmetric ruthenium tetramers, [(Δ-Ru(phen)$_2$(tpphz))$_3$-Δ-Ru][PF$_6$]$_8$ (ΔΔ$_3$-**1**), ΛΛ$_3$-**1**, ΔΛ$_3$-**1**, and ΛΛ$_3$-**1**, are described herein. These complexes represent the highest nuclearity ruthenium oligomers based on bidentate type ligands prepared in diastereomerically and enantiomerically pure form.

Results and Discussion

Synthesis. The synthesis of ΔΛ$_3$-**1**, shown in Scheme 2, is representative for all D_3 isomers of **1**. Enantiopure metal-complex-building blocks, Δ-[Ru(phendione)$_3$][PF$_6$]$_2$ (Δ-**2**) and 3.1 equiv of Λ-[Ru(phen)$_2$(phendiamine)][PF$_6$]$_2$ (Λ-**3**) (where phen is 1,10-phenanthroline, phendione is 1,10-phenanthroline-5,6-dione, and phendiamine is 1,10-phenanthroline-5,6-diamine), are linked along the 2-fold axes of the complexes using condensation reactions between the *o*-diamine and *o*-dione functions to form a pyrazine ring between complexes. The result is a rigid D_3-symmetric trigonal-propeller-shaped molecule (ΔΛ$_3$-**1** in Scheme 2) with an estimated diameter of 3.4 nm. Theoretically, the product has a maximum of 2^4 isomers which in this case is lowered to 8, due to the trigonal symmetry. The four D_3-symmetric isomers are easily obtained by a straightforward coupling of Δ(or Λ)-**2** with three identical Δ(or Λ)-**3** complexes at the edge. Preparation of the four C_2-symmetric isomers was not attempted; however, a statistical mixture of all isomers (*mix*-**3**) was obtained from the reaction of racemic **2** and racemic **3**. Because the ring formation gives a planar-symmetric (D_2) tpphz ligand, the symmetry of the monomer's 2-fold axes is maintained and rotational and conformational motion is restricted.[44] This fixes the Ru$_{central}$ to Ru$_{terminal}$ distance to 12.7 Å, as determined from a structural analysis of the related dimer [(bpy)$_2$Ru(tpphz)Ru(bpy)$_2$][NO$_3$]$_4$,[45] and gives calculated Ru$_{terminal}$ to Ru$_{terminal}$ distances at 23 Å.

(32) Newkome, G. R.; Cardullo, F.; Constable, E. C.; Moorefield, C. N.; Thompson, A. M. W. C. *J. Chem. Soc., Chem. Commun.* **1993**, 925.

(33) Newkome, G. N.; Güther, R.; Moorefield, C. N.; Cardullo, F.; Echegoyen, L.; Pérez-Cordero, E.; Luftmann, H. *Angew. Chem., Int. Ed. Engl.* **1995**, *34*, 2023.

(34) Constable, E. C.; Cargill Thompson, A. M. W.; Harveson, P.; Macko, L.; Zehnder, M. *Chem. Eur. J.* **1995**, *1*, 360.

(35) Constable, E. C.; Harverson, P.; Oberholzer, M. *Chem. Commun.* **1996**, 1821.

(36) Constable, E. C.; Harverson, P. *Chem. Commun.* **1996**, 33.

(37) Sauvage, J.-P.; Collin, J.-P.; Chambron, J.-C.; Guillerez, S.; Coudret, C.; Balzani, V.; Barigelletti, F.; De Cola, L.; Flamigni, L. *Chem. Rev.* **1994**, *94*, 993.

(38) Meyer, T. J. *Acc. Chem. Res.* **1989**, *22*, 163.

(39) Juris, A.; Balzani, V.; Barigelletti, F.; Campagna, S.; Belser, P.; Von Zelewsky, A. *Coord. Chem. Rev.* **1988**, 85.

(40) Rutherford, T. J.; Quagliotto, M. G.; Keene, F. R. *Inorg. Chem.* **1995**, *34*, 3857.

(41) HAT (1,4,5,8,9,12-hexaazatriphenylene) and PHAT (9,10,19,20,-29,30-hexaazohexapyrido[3,2-*a*:2′,3′-*c*:3″,2″-*k*:2‴,3‴-*m*:3⁗,2⁗-*u*:2″‴,3″‴-*x*]trinaphthylene) are planar-trigonally symmetric (D_{3h}) tritopic ligands. See refs 29 and 42 for triruthenium complexes of these ligands.
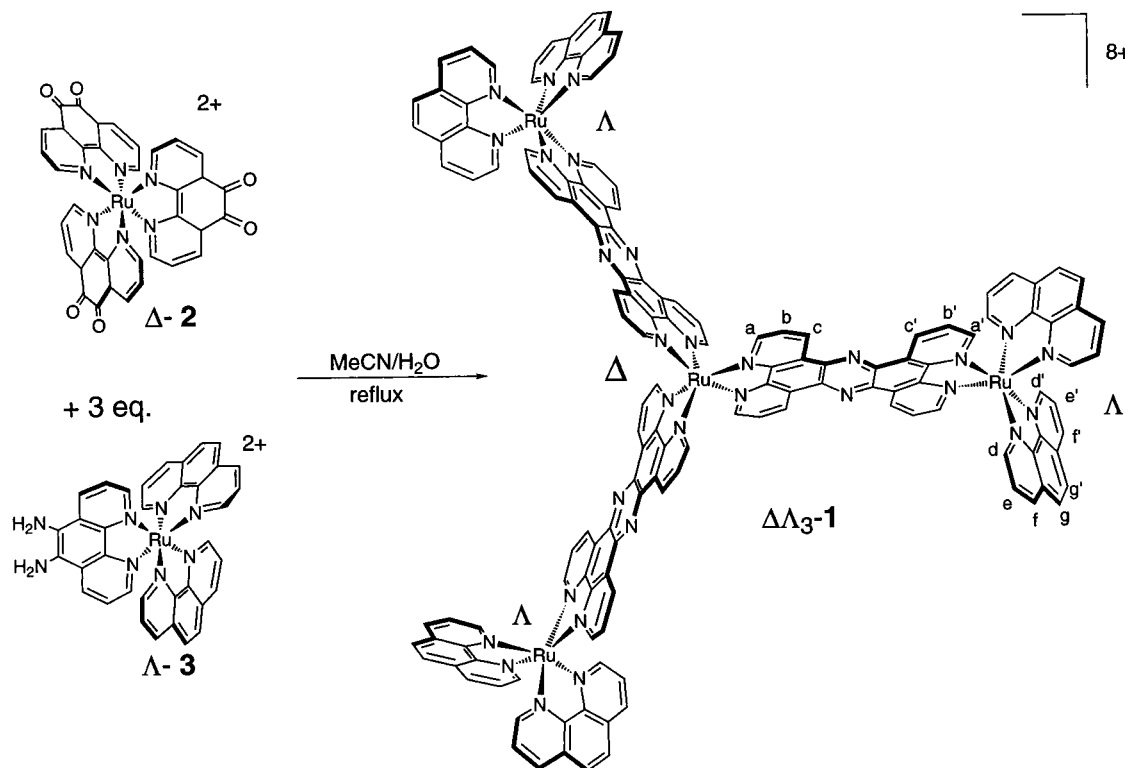
(42) Masschelein, A.; Kirsch-De Mesmaeker, A.; Verhoeven, C.; Nasielski-Hinkens, R. *Inorg. Chim. Acta* **1987**, *129*, L13.

(43) Tzalis, D.; Tor, Y. *Chem. Commun.* **1996**, 1043.

(44) Some slight bending and twisting of the tpphz bridge was observed in the cyrstal structure of [(bpy)$_2$Ru(tpphz)Ru(bpy)$_2$][NO$_3$]$_4$ (ref 45).

(45) Bolger, J.; Gourdon, A.; Ishow, E.; Launay, J.-P. *J. Chem. Soc., Chem. Commun.* **1995**, 1799.

Scheme 2

Each phenazine-coupling reaction is approximately 95% efficient as indicated by NMR data on the crude product; however, after chromatography isolated yields are typically between 65% and 70%. This is a considerable improvement over the yields observed for ligand displacement reactions of chiral $[Ru(L-L)_2(L)_2]^{2+}$ complexes (where L-L is phen or bpy and L is py or CO) with multitopic bidentate ligands.[27,28,40] For example, coupling between three Δ-$[Ru(phen)_2(py)_2]^{2+}$ and HAT type ligands gave the trimers in only 10−25% isolated yields.[29]

Surprisingly, the major impurity (isolated in >10% yield based on **3**) was found to be the dimer **4**. This product can be explained by oxidative formation of [Ru(phen)$_2$(1,10-phenanthroline-5,6-diimine)$_2$]$^{2+}$ which couples with **3** to give the dimer **4** and NH_3. The dimer and tetramer were not separable by standard chromatography (silica or alumina); however, they were separable by HPLC using a strong cation-exchange resin (Hamilton PRP-X200). The product **1** is selectively absorbed onto the resin with a low-salt/acid mobile phase which elutes all the low-charge species (≤+4) and then eluted by switching to a high-salt/acid mobile phase. The cation (8+) **1** is readily soluble in acetonitrile and acetone as the hexafluorophosphate salt and in water, methanol, or ethanol as the chloride salt.

Characterization. The D_3 symmetry for **1** is clearly evident in the NMR data. Of the 84 H atoms in the structure, only 14 are symmetrically inequivalent and, by analysis, only 12 are magnetically inequivalent. The 1D and COSY ^{1}H NMR data for the $\Lambda\Delta_3$ isomer are provided in Figure 1 (proton-labeling scheme is indicated in Scheme 2). The proton assignments shown in Figure 1 are based on the coupling patterns established by COSY spectra and by comparison with related compounds. In general, the doublets furthest downfield can be attributed to H_c and $H_{c'}$ as opposed to H_f and $H_{f'}$ in accordance with the literature assignments for complexes of phen, dppz, and tpphz type ligands.[26,46,47] Some ambiguity arises in the assignments
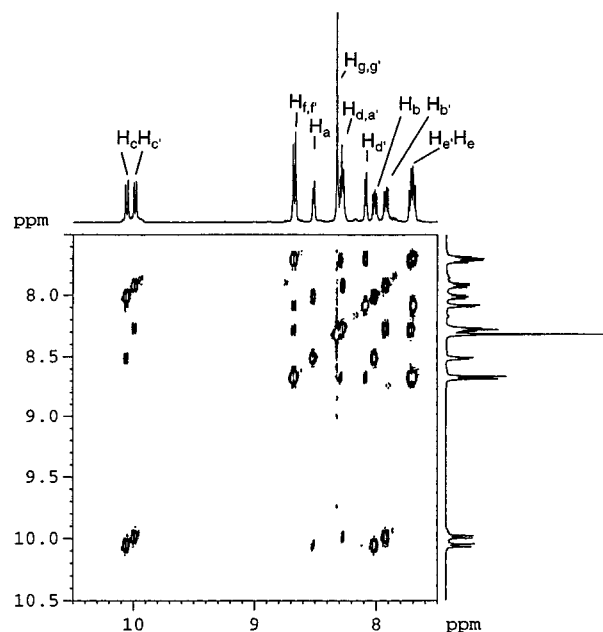
(46) Bolger, J.; Gourdon, A.; Ishow, E.; Launay, J.-P. *Inorg. Chem.* **1996**, *10*, 2937.

Figure 1. 1D and COSY ^{1}H NMR spectrum of $\Lambda\Delta_3$-**1** (PF$_6^-$ salt, 400 MHz in CD$_3$CN).

of closely related protons, such as the tpphz inner protons (H_a, H_b, H_c) and outer protons ($H_{a'}$, $H_{b'}$, $H_{c'}$). COSY data reveal the peaks at 8.46 (d), 7.96 (dd), and 10.01 (d) ppm form one AMX-coupled set and the peaks at 8.24 (d), 7.87 (dd), and 9.94 (d) ppm form another A′M′X′-coupled set. The latter set is assigned as the outer protons ($H_{a'}$, $H_{b'}$, $H_{c'}$) by comparison with the chemical shifts observed at 8.21 (d), 7.88 (dd), and 9.94 (d) ppm for the related positions on $\Delta\Delta$-**4** which we believe better simulate the outer ($H_{a'}$, $H_{b'}$, $H_{c'}$) environment.[26]

The terminal phen ligands in **1** show interesting NMR behavior. The Hd proton *cis* to the tpphz ligand lies over the

(47) Dupureur, C. M.; Barton, J. K. *J. Am. Chem. Soc.* **1994**, *116*, 10286.
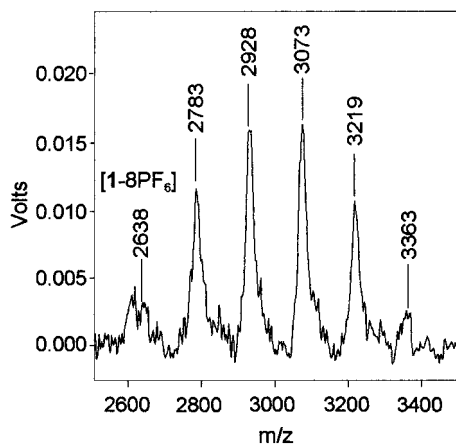
Figure 2. Molecular ion region of the MALDI-TOF mass spectrum of $\Lambda\Delta_3$-**1**.

Figure 3. Overlaid circular dichroism spectra of $\Lambda\Lambda_3$-**1** (bold solid line), $\Delta\Lambda_3$-**1** (solid line), $\Lambda\Delta_3$-**1** (dotted line), and $\Delta\Delta_3$-**1** (bold dotted line) PF_6^- salt in acetonitrile at room temperature (2.0×10^{-6} M).

tpphz ring and is shifted downfield by 0.22 ppm relative (8.24 ppm) to the *trans* $H_{d'}$ proton which lies over a phen ring (8.04 ppm), reflecting the relative deshielding ability of the two ligands when a H atom is oriented directly over the aromatic ring system. Similar behavior is observed in the isomers of **4** and [(phen)$_2$Ru(bipyrimidine)Ru(phen)$_2$][PF$_6$]$_2$.[28] $H_{d'}$ is assigned on the basis of its chemical shift (8.04 ppm) compared to the related protons in [Ru(phen)$_3$]$^{2+}$ which are found at 8.09 ppm. The next-nearest neighbors H_e and $H_{e'}$ are only slightly differentiated ($\Delta\delta = 0.02$ ppm) while the pairs H_f, $H_{f'}$ and H_g, $H_{g'}$ were not resolved at fields up to 500 MHz. Apparently, the electronic and structural similarity of tpphz with the terminal phen ligands is similar enough that there is little distinction by NMR criterion of *cis*- and *trans*-related positions on the phen ligands past H_f and $H_{f'}$.

^{13}C NMR analyses of these complexes showed similar effects. Only 21 resonances are observed for 24 symmetrically inequivalent carbons. An HMQC experiment established the identity of the 14 protonated carbons (data provided as Supporting Information). As observed in the proton experiment, the pseudosymmetrically related (*cis* and *trans*) carbons bound to the isochronous pairs H_f, $H_{f'}$ and H_g, $H_{g'}$ are not resolved whereas the carbons correlated to the pair H_e, $H_{e'}$ are separated by 0.07 ppm and the H_d, $H_{d'}$ pair by 0.31 ppm.

As observed in the dimers ($\Delta\Delta$-**4**, $\Lambda\Lambda$-**4**, and $\Delta\Lambda$-**4**), all isomers of **1** give virtually identical NMR spectra. Even the sample, *mix*-**1**, gave sharp indistinguishable NMR spectra. We suggest the large distances between stereocenters is responsible and point out that even at much closer distances, chemically distinct nuclei (i.e., with *cis* and *trans* positions) are often indistinguishable by NMR. This situation is both fortuitous, in that it permits the synthetic routes to be worked out with racemic starting materials, and detrimental, in that it prevents determination of diastereomeric purity by NMR. Fortunately, CD spectra can help determine the latter.

The tetrameric structure of the cation [Ru$_4$C$_{144}$H$_{84}$N$_{30}$]$^{8+}$ (**1**) was further established by matrix-assisted laser desorption ionization (MALDI) mass spectrometry.[48] Figure 2 shows an expansion of the molecular ion region of the MALDI mass spectrum of the [M(PF$_6$)$_n$]$^+$ (where $n = 0-5$). The small peak at 2638 is assigned to the [M − 8PF$_6$]$^+$ cation which has a calculated average *m/z* of 2638.7.[49] Resolution in this mass spectrum is insufficient to determine if the ion observed is the
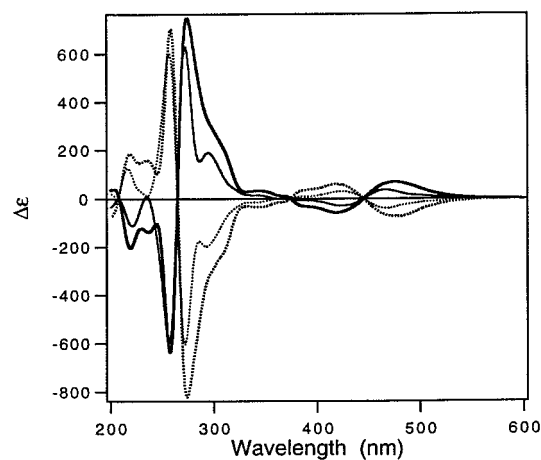
protonated molecule ion (typical of MALDI) or the radical cation. Clearly distinguishable ion signals are also observed at *m/z* 2783 [M − 7PF$_6$]$^+$, 2928 [M − 6PF$_6$]$^+$, 3073 [M − 5PF$_6$]$^+$, 3218 [M − 4PF$_6$]$^+$, and 3363 [M − 3PF$_6$]$^+$. It is unlikely that these species have undergone varying degrees of reduction and PF$_6^-$ retention such that each species achieves an overall +1 charge, particularly since other charge states of the Ru$_4$ complex are not observed. A more consistent explanation is that each of these species represents protonated, fully reduced Ru$_4$ complexes which have undergone dissociative loss of varying numbers of PF$_6^-$ counterions. Regardless, these species all invoke the formation of highly reduced Ru$_4$ singly charged cations which, while unusual, is not unprecedented. Neutral and partially reduced [Ru(bpy)$_3$]$^{1+/0}$ type complexes have been electrocrystallized from solution and structurally characterized.[50,51] Similarly reduced species were observed in FABS[52] and MALDI[33,35] mass spectroscopy experiments in related M − polypyridyl systems. For these systems, the reducing electrons are postulated to reside in the low-lying LUMOs centered largely on the polypyridyl ligands.

Circular dichroism spectra are required to clearly reveal enantiomeric and diastereomeric relationships between the isomers and to demonstrate the retention of optical activity by the chiral centers. CD spectra of the four isomers, shown in Figure 3, show the expected mirror image relationship between the two pairs of enantiomers $\Delta\Delta_3$-**1**, $\Lambda\Lambda_3$-**1** and $\Lambda\Delta_3$-**1**, $\Delta\Lambda_3$-**1**. An approximate additive relationship between the number and type of chromophores and the magnitude of the molar ellipticity is observed in the CD. $\Lambda\Lambda_3$-**1** and $\Delta\Lambda_3$-**1** both exhibit positive Cotton effects as the lowest energy transitions at 476 and 466 nm, respectively, but differ in magnitude. The value of +68 at 476 nm for $\Lambda\Lambda_3$-**1** is approximately double that for $\Delta\Lambda_3$-**1** (+35 at 465 nm) which reflects the net number of chiral chromophores (i.e., four Λ for $\Lambda\Lambda_3$-**1** and two Λ for $\Delta\Lambda_3$-**1**) with apparently little regard for the tertiary arrangement of these stereocenters. Similar data are observed for $\Delta\Delta_3$-**1** and $\Lambda\Lambda_3$-**1**. Each chromophore adds approximately ±17 molar ellipticity units at the low-energy peak which compares well with the values observed in Λ-[Ru(phen)$_3$]$^{2+}$ (+21 at 467 nm) and Λ-[Ru(phen)$_2$(phendione)]$^{2+}$ (+17 at 470 nm). Similar effects were observed in chiral dimers[26,30] and trimers.[29]

(48) Hillenkamp, F.; Karas, M.; Beavis, R. C.; Chait, B. T. *Anal. Chem.* **1991**, *63*, 1193A.

(49) Average molecular weight calculated using the program IsoPro, written by M. W. Senko at the National High Magnetic Field Laboratory, Tallahassee, FL.
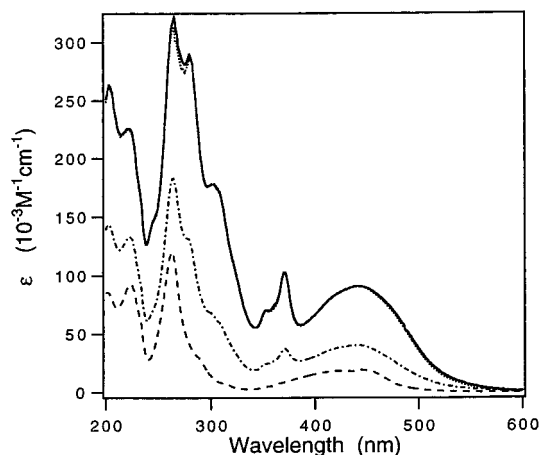
(50) Pérez-Cordero, E.; Campagna, C.; Echegoyen, L. *Angew. Chem., Int. Ed. Engl.* **1997**, *36*, 137.

(51) Pérez-Cordero, E.; Brady, N.; Echegoyen, L.; Thummel, R.; Hung, C.-Y.; Bott, S. G. *Chem. Eur. J.* **1996**, *2*, 781.

(52) Denti, G.; Serroni, S.; Sindona, G.; Uccella, N. *J. Am. Soc. Mass. Spectrom.* **1993**, *4*, 306.

Figure 4. Overlaid electronic spectra of $\Delta\Delta_3$-**1** (solid line), $\Delta\Lambda_3$-**1** (dotted line), $\Delta\Delta$-**4** (dot−dash line), and [Ru(phen)$_3$][PF$_6$]$_2$ (dashed line) PF$_6^-$ salt in acetonitrile at room temperature (2.0 × 10^{-6} M).

Absorption spectra for all four isomers in MeCN were identical within experimental error indicating no electronic differences between diastereomers, consistent with the NMR data. The spectra of two diastereomers are overlaid in Figure 4 showing the similarity of two spectra and indicating the intense molar extinction coefficients in the visible and UV. For comparison, the electronic data for [Ru(phen)$_3$][PF$_6$]$_2$ and $\Delta\Delta$-**4** are included in Figure 4. As was observed in the CD spectra, peak molar extinction coefficients for these complexes approximate the values anticipated simply by adding up the extinction values for four independent chromophores. For example, the molar extinction coefficients of [Ru(phen)$_3$][PF$_6$]$_2$, $\Delta\Delta$-**4**, and $\Delta\Delta_3$-**1** at approximately 450 nm are 19 000, 39 700, and 87 900 M^{-1} cm^{-1}, respectively. These values correspond well with those observed for the related complexes [Ru(phen)$_2$-(tpphz)]$^{2+}$ and [(bpy)$_2$Ru(tpphz)Ru(bpy)$_2$]$^{4+}$ at 19 700 and 36 000 M^{-1} cm^{-1}, respectively.[46] The broad low-energy absorption at 400−500 nm is actually composed of multiple absorptions attributed to the Ru → phen and Ru → tpphz MLCTs.[46,53] The two sharp absorptions at 372 and 354 nm are only observed in systems containing the tpphz ligand and have been assigned as the tpphz $n \to \pi^*$ and $\pi \to \pi^*$ transitions in related works.[46,54] The absence of the intense shoulders at 279 and 300 nm in [Ru(phen)$_3$]$^{2+}$ suggests these peaks are tpphz $\pi \to \pi^*$ transitions.

Conclusions

This work demonstrates the viability of using coupling reactions between coordinated ligands in chiral metal complexes as a completely modular approach to the stereospecific synthesis of multinuclear metal complexes. In summary, four major advantages over existing methods result from this work. First, we avoid any reaction at the metal stereocenter thereby retaining the local stereochemistry and forming a single diastereomeric product which can be completely characterized. Second, the resulting aromatic bridge is symmetrical, rigid, and stable and provides an electronic conduit between metal centers. Third, by extending the pyrazine-coupling reaction along all three axes of the homoleptic monomer [Ru(phendione)$_3$]$^{2+}$, the full D_3 symmetry is utilized, resulting in a nanoscopic product of exceptionally high symmetry (for a chiral molecule). Fourth, the modular design utilized in this synthesis permits easy access to most desired stereoisomers and/or heterometallic structures.

Our synthetic approach represents a definitive solution to the problem of constructing isomerically pure supramolecular structures and should be extendible for the syntheses of higher nuclearity complexes, dendrimers, and polymers. This work will allow us to probe the effect of stereochemistry on the photophysical and energy-transfer properties of these and related assemblies, and such studies are currently underway. These first-generation dendrimers also contain stereochemically well-defined molecular clefts owing to the optical purity and conformational rigidity of the overall structure and may ultimately find uses as chiral host complexes and chiral catalysts.

Experimental Section

Materials. The enantiomers of [Ru(phen)$_2$(1,10-phenanthroline-5,6-dione)][PF$_6$]$_2$ were prepared and resolved into Λ- and Δ-optical isomers according to the literature procedures.[53] Λ- and Δ-[Ru(phendione)$_3$]-[PF$_6$]$_2$ were generated by oxidation of respective tris-phenanthroline complexes[55,56] by a slight modification of the literature method.[57] Λ- and Δ-[Ru(phen)$_2$(phendiamine)][PF$_6$]$_2$ were prepared from resolved [Ru(phen)$_2$(phendione)][PF$_6$]$_2$ as reported in our earlier publication[26] and were further purified on neutral alumina using acetonitrile containing 10 mg/mL NH$_4$PF$_6$ as an eluent. All other chemicals and solvents used were of reagent grade and used without further purification. All the reactions were carried out under N$_2$ gas and protected from direct light to prevent photochemical degradation.

Instrumentation. ^{1}H and ^{13}C NMR spectra were obtained on a Bruker MSL-300, Bruker AVANCE 400, or JEOL Eclipse Plus 500 MHz spectrometer using CD$_3$CN as the solvent. Chemical shifts are given in ppm and referenced to TMS. CD spectra were recorded on a Jasco-710 spectrophotometer in MeCN. UV−visible data were obtained on a Hewlett-Packard HP8453A spectrophotometer in MeCN. Semipreparative scale cation-exchange chromatography was performed with a Waters model 590 HPLC pump with a 1 mL injection loop, a Hamilton PRP-X200 column (10 × 250 mm), and a Spectra variable wavelength UV−vis detector. Samples for MALDI mass spectroscopic analysis were prepared by cocrystallizing 10 μL of **1** in acetone (1 mg/mL), 15 μL of 10% trifluoroacetic acid in methanol, and 15 μL of α-cyano-4-hydroxycinnamic acid in methanol (15 mg/mL) on the surface of a stainless steel direct insertion probe. Samples were introduced to an in-house constructed, linear time-of-flight mass spectrometer operated with a continuous 18 kV accelerating potential in the ion source region. Laser desorption was performed at 337 nm at intensities just above threshold for ion formation. After acceleration, laser-desorbed ions were separated in a 1.0 m drift tube and detected by a dual microchannel plate detector operated at −4.0 kV of post acceleration.

Synthesis of Tetranuclear Complexes [(Ru(phen)$_2$(tpphz))$_3$Ru]-[PF$_6$]$_8$ (1). General Procedure. A 0.025 g (0.024 mmol) portion of the appropriate (*rac* or Λ or Δ)-[Ru(phendione)$_3$][PF$_6$]$_2$ (**2**) and 0.073 g (0.076 mmol) of the appropriate (*rac* or Λ or Δ)-[Ru(phen)$_2$-(phendiamine)][PF$_6$]$_2$ (**3**) were dissolved in 15 mL of a 3:2 acetonitrile−water mixture. The reaction flask was covered with aluminum foil and refluxed under N$_2$ gas for 8−10 h. The acetonitrile was removed in vacuo, resulting in the precipitation of an orange complex. Addition of 10 mL of water containing 0.2 g of NH$_4$PF$_6$ completed the precipitation which was stirred for an additional 15 min. The mixture was cooled, filtered, washed twice with 5 mL each of water, and dried in vacuo at 60 °C. The product was further purified by HPLC using a cation-exchange column and tunable UV−vis detector (440 nm). The initial mobile phase was 70:30 acetonitrile−0.3 N aqueous HNO$_3$ (8 mL/min) which was used to elute all the low-charge species. The product was eluted by switching to a 70:30 acetonitrile−6 N aqueous HNO$_3$ mobile phase. Addition of excess NH$_4$PF$_6$ and subsequent neutralization of the nitric acid with NaOH (30%) resulted in the

(53) Hiort, C.; Lincoln, P.; Nordén, B. *J. Am. Chem. Soc.* **1993**, *115*, 3448.

(54) Amouyal, E.; Homsi, A.; Chambron, J.-C.; Sauvage, J.-P. *J. Chem. Soc., Dalton Trans.* **1990**, 1841.

(55) Dwyer, F. P.; Gyarfas, E. C. *J. Proc. R. Soc. New South Wales* **1949**, *83*, 170.

(56) Maloney, D. J.; MacDonnell, F. M. *Acta Crystallogr., Sect. C* **1997**, 705.

(57) Gillard, R. D.; Hill, R. E. E. *J. Chem. Soc., Dalton Trans.* **1974**, 1217.

acetonitrile−aqueous salt solution phase separating with the product in the organic phase. Removal of the MeCN in vacuo and addition of water gave the purified product as an orange powder, which was filtered, washed twice with 5 mL each of water, and dried *in vacuo* at 60 °C. Typical yield was 0.065 g (68%).

[(Λ-Ru(phen)$_2$(tpphz))$_3$-Λ-Ru][PF$_6$]$_8$ (ΛΛ$_3$-1): ^{1}H NMR (δ) 10.01 (d, 6H, J = 8.40 Hz), 9.95 (d, 6H, J = 8.23 Hz), 8.63 (d, 12H, J = 8.28 Hz), 8.46 (d, 6H, J = 5.56 Hz), 8.28 (s, 12H), 8.23 (m, 12H), 8.04 (d, 6H, J = 5.29), 7.96 (dd, 6H, J_1 = 8.40 Hz, J_2 = 5.49 Hz), 7.87 (dd, 6H, J_1 = 8.18 Hz, J_2 = 5.41 Hz), 7.66 (dd, 6H, J_1 = 8.18 Hz, J_2 = 5.32 Hz), 7.64 (dd, 6H, J_1 = 8.18 Hz, J_2 = 5.33 Hz); ^{13}C NMR (δ) 156.30, 155.97, 154.24, 153.90, 151.88, 151.72, 146.79, 141.53, 141.45, 137.94, 135.32, 134.80, 132.02, 131.16, 130.90, 129.03, 128.45, 128.26, 126.83; UV−vis [λ_{max}, nm ($\epsilon \times 10^{-4}$ M^{-1} cm^{-1})] 203 (25.9), 222 (22.1), 265 (30.3), 279 (27.4), 301(17.1), 354 (6.68), 372 (9.84), 442 (8.65); CD [λ_{max}, nm ($\Delta\epsilon$)] 218 (−202), 234 (−137), 258 (−637), 274 (+750), 305 (+238), 344 (+31.4), 363sh (+11.5), 390sh (−32.8), 417 (−57.5), 476 (+68.1).

[(Δ-Ru(phen)$_2$(tpphz))$_3$-Δ-Ru][PF$_6$]$_8$ (ΔΔ$_3$-1): ^{1}H NMR (δ) 10.01 (d, 6H, J = 7.59 Hz), 9.95 (d, 6H, J = 7.46 Hz), 8.62 (d, 12H, J = 8.53 Hz), 8.46 (d, 6H, J = 5.28 Hz), 8.28 (s, 12H), 8.23 (m, 12H), 8.04 (d, 6H, J = 5.85 Hz), 7.96 (dd, 6H, J_1 = 8.40 Hz, J_2 = 5.70 Hz), 7.87 (dd, 6H, J_1 = 8.25 Hz, J_2 = 5.44 Hz), 7.66 (dd, 6H, J_1 = 8.13 Hz, J_2 = 5.30 Hz), 7.64 (dd, 6H, J_1 = 8.16 Hz, J_2 = 5.31 Hz); ^{13}C NMR (δ) 156.28, 155.97, 154.24, 153.88, 151.84, 151.68, 148.77, 148.71, 141.52, 141.42, 137.91, 135.28, 134.75, 131.98, 131.02, 130.88, 129.00, 128.44, 128.22, 126.81; UV−vis [λ_{max}, nm ($\epsilon \times 10^{-4}$ M^{-1} cm^{-1})] 203 (26.4), 222 (22.6), 265 (32.2), 279 (29.0), 301 (17.8), 354 (7.01), 372 (10.3), 442 (9.10); CD [λ_{max}, nm ($\Delta\epsilon$)] 218 (+185), 234 (+158), 258 (+705), 274 (−822), 305 (−247), 344 (−33.7), 363sh (−14.6), 390sh (+34.9), 417 (+59.5), 476 (−73.2).

[(Δ-Ru(phen)$_2$(tpphz))$_3$-Λ-Ru][PF$_6$]$_8$ (ΛΔ$_3$-1): ^{1}H NMR (δ) 10.01 (d, 6H, J_1 = 8.33 Hz, J_2 = 1.23 Hz), 9.94 (d, 6H, J_1 = 8.27 Hz, J_2 = 1.20 Hz), 8.63 (d, 12H, J = 8.21 Hz), 8.46 (d, 6H, J_1 = 5.38 Hz, J_2 = 1.28 Hz), 8.27 (s, 12H), 8.25 (m, 12H), 8.04 (d, 6H, J_1 = 5.33 Hz, J_2 = 1.20 Hz), 7.96 (dd, 6H, J_1 = 8.31 Hz, J_2 = 5.45 Hz), 7.87 (dd, 6H, J_1 = 8.30 Hz, J_2 = 5.50 Hz), 7.67 (dd, 6H, J_1 = 8.29 Hz, J_2 = 5.37 Hz), 7.63 (dd, 6H, J_1 = 8.29 Hz, J_2 = 5.41 Hz); ^{13}C NMR (δ) 156.27, 155.95, 154.17, 153.88, 151.87, 151.68, 148.74, 141.49, 141.39, 137.89, 135.31, 134.70, 131.98, 131.11, 130.85, 128.98, 128.41, 128.20, 126.83; UV−vis [λ_{max}, nm ($\epsilon \times 10^{-4}$ M^{-1} cm^{-1})] 203 (25.6), 222 (22.1), 265 (30.6), 279 (27.7), 301 (17.2), 354 (6.82), 372 (10.0), 442 (8.79); CD

[λ_{max}, nm ($\Delta\epsilon$)] 216 (+125), 257 (+602), 272 (−604), 292 (−198), 342sh (−15.3), 388sh (+9.13), 422 (+29.3), 465 (−38.4).

[(Λ-Ru(phen)$_2$(tpphz))$_3$-Δ-Ru][PF$_6$]$_8$ (ΔΛ$_3$-1): ^{1}H NMR (δ) 10.01 (d, 6H, J_1 = 8.28 Hz, J_2 = 1.20 Hz), 9.94 (d, 6H, J_1 = 8.34 Hz, J_2 = 1.27 Hz), 8.62 (d, 12H, J = 8.20 Hz), 8.46 (d, 6H, J_1 = 5.25 Hz, J_2 = 1.14 Hz), 8.27 (s, 12H), 8.25 (m, 12H), 8.04 (d, 6H, J_1 = 5.25 Hz, J_2 = 1.17 Hz), 7.96 (dd, 6H, J_1 = 8.31 Hz, J_2 = 5.37 Hz), 7.87 (dd, 6H, J_1 = 8.30 Hz, J_2 = 5.44 Hz), 7.66 (dd, 6H, J_1 = 8.29 Hz, J_2 = 5.40 Hz), 7.64 (dd, 6H, J_1 = 8.32 Hz, J_2 = 5.41 Hz); ^{13}C NMR (δ) 156.30, 155.99, 154.22, 153.92, 151.85, 151.71, 148.73, 141.53, 141.43, 137.92, 135.31, 134.77, 132.00, 131.14, 130.89, 129.01, 128.82, 128.24, 126.82; UV−vis [λ_{max}, nm ($\epsilon \times 10^{-4}$ M^{-1} cm^{-1})] 203 (26.1), 222 (22.4), 265 (31.3), 279 (28.6), 301 (17.9), 354 (6.92), 372 (10.2), 442 (9.03); CD [λ_{max}, nm ($\Delta\epsilon$)], 216 (−112), 257 (−594), 272 (+630), 292 (+190), 342sh (+13.8), 390sh (−8.12), 422 (−29.0), 465 (+35.5).

***mix*-[(Ru(phen)$_2$(tpphz))$_3$Ru][PF$_6$]$_8$ (*mix*-1):** ^{1}H NMR (δ) 10.03 (d, 6H, J = 8.55 Hz), 9.96 (d, 6H, J = 7.60 Hz), 8.64 (d, 12H, J = 8.40 Hz), 8.47 (d, 6H, J = 8.40 Hz), 8.28 (s, 12H), 8.26 (m, 12H), 8.05 (d, 6H, J = 5.18 Hz), 7.96 (dd, 6H, J_1 = 8.28 Hz, J_2 = 5.54 Hz), 7.89 (dd, 6H, J_1 = 8.23 Hz, J_2 = 5.48 Hz), 7.66 (m, 12H); ^{13}C NMR (δ) 156.30, 155.98, 154.20, 153.88, 151.84, 151.68, 148.77, 148.71, 141.49, 141.40, 137.90, 135.00, 134.75, 131.97, 131.11, 130.85, 128.99, 128.42, 128.20, 126.85. Anal. Calcd for C$_{144}$H$_{96}$F$_{48}$N$_{30}$O$_6$P$_8$Ru$_4$ (*mix*-1·6H$_2$O): C, 44.27; H, 2.48; N, 10.76. Found: C, 44.11; H, 2.37; N, 10.32.

Supporting Information Available: HMQC NMR spectrum of ΛΔ$_3$-**1** (1 page). See any current masthead page for ordering and Internet access instructions.